Renewable and Sustainable Energy Reviews 15 (2011) 4818–4828

Contents lists available at SciVerse ScienceDirect

Renewable and Sustainable Energy Reviews

journal homepage: www.elsevier.com/locate/rser

Study on small signal stability of microgrids: A review and a new approach

Zheng Zeng [1], Huan Yang *, Rongxiang Zhao [2]

College of Electrical Engineering, Zhejiang University, 310027 Hangzhou, Zhejiang Province, China

ARTICLE INFO

Article history:
Received 28 February 2011
Accepted 5 July 2011
Available online 15 September 2011

Keywords:
Microgrid
Small signal stability
Singular Entropy Matrix Pencil

ABSTRACT

Microgrid is an effective concept for distributed renewable energies connecting to utility grid. However, enormous challenges have also been brought into the microgrids study considering the intermittence, randomness characteristics of renewable energies. As a result, the power generations of distributed generators fluctuate frequently. Furthermore, it is difficult to obtain the parameters of microgrids accurately. Thus, the study on small signal stability of microgrids is especially important. This paper presents a review of exiting small signal stability methods for microgrids. Besides, a new approach based on Singular Entropy and Matrix Pencil is proposed. Meanwhile, its validity and effectiveness are confirmed by some examples compared with Prony algorithm. Then, the proposed method is also applied into a microgrid with an improved droop control strategy. Finally, a framework based on the proposed method for small signal stability, warning and emergency control online in microgrids is available.

Contents

1. Introduction

Recently, the shortage of fossil fuels, vulnerability of large grid and the power blackouts caused by it have been more and more serious [1–3]. Therefore, distributed and renewable energies such as wind, solar and so on gained more and more interests [4–6]. However, because of their intermittence, randomness and uncertainty caused by meteorological factors, it is hard to connect renewable energy sources to utility grid directly [7–10]. By integrating distributed and renewable sources, energy storage devices, a variety of loads, data acquisition and supervisory control devices, microgrids realize the interface between the distributed renewable sources and utility grid [11–13].

At present, the researches on microgrids mainly focus on the optimal design of system capacity [14], power generation operation and control [15–18], system modeling and simulation [19–23], power quality [24,25] and so on, while rarely on the stability [26,27]. However, stable and reliable power supply to loads or utility grid is the basic function of microgrids. So, study on stability of microgrids is very necessary and important. Unlike transmission

* Corresponding author. Tel.: +86 13588846066.
E-mail addresses: zengerzheng@zju.edu.cn (Z. Zeng), yanghuan@zju.edu.cn (H. Yang), rongxiang@zju.edu.cn (R. Zhao).
[1] Tel.: +86 13567123512.
[2] Tel.: +86 13906508946.

1364-0321/$ – see front matter © 2011 Elsevier Ltd. All rights reserved.
doi:10.1016/j.rser.2011.07.069

Nomenclature

P_i, Q_i	active power or reactive power output of the ith distributed generator (DG), DG_i, whose output apparent power is $S_i = P_i + jQ_i$. Especially, P_{refi} (Q_{refi}) is its reference value. Similarly, P_g (Q_g) and S_g are the ones supplied by utility grid
$\tilde{P}$, $\tilde{Q}$	active power or reactive power after digital filter in inverter controller
P_{Li}, Q_{Li}	active or reactive power demand of the ith load
k_{pp}, k_{pi}	proportion and integration coefficient of DG_i for active power droop control
k_{qp}, k_{qi}	proportion and integration coefficient of DG_i for reactive power droop control
r, x_L	resistance and inductance of line per kilometer
ω_0	rated angular frequency of the microgrid
E_0	rated potential of DG
$\boldsymbol{V}_{ref}$	three-phase reference voltage vector of DG
$\boldsymbol{E}_p$	potential of DG injected into the microgrid
T_s	sample time of raw data or sampled data for small signal stability modes extraction
y	raw data acquisited from microgrid, and $y(i)$ (i = 1, 2, . . ., N) is its ith point, where N is the length of it
Y	formed Hankel matrix by raw data
E_k, ΔE_k, $\Delta E'_k$	the kth Singular Entropy, Singular Entropy Increment and Differential of Singular Entropy Increment, respectively
n	modal order of raw data
λ_i, f_i, ξ_i	the eigenvalue, frequency and damping ratio of ith mode
SNR	signal noise ratio

network or distribution network, microgrids can operate in isolated mode or interconnected mode [12]. This feature brings out a serious challenge to stability analysis of microgrids. Stability of microgrids also includes two parts. One is small signal stability (SSS) in small disturbances sense, and the another is the transient stability in large disturbances sense. Except for large disturbances, the power outputs of wind turbines, photovoltaic arrays and other renewable sources are time-variant, which can be regarded as small disturbances. What is more, they may couple with load fluctuations too. Thus, these kinds of small power fluctuations are so frequent that they affect the operation status of microgrids constantly. In a word, the difficulty and necessity of study on SSS of microgrids is evident.

This paper reviews the current approaches for SSS of microgrid. Besides, an improved Matrix Pencil combined with Singular Entropy is presented and applied to extract the SSS modes of microgrids. The paper is organized as follows. In Section 2, a review of exciting and prosiable methods for SSS of microgrids is available. In Section 3, the basic mathematical model of Singular Entropy Matrix Pencil is proposed. In addition, the microgrid structure and an improved control strategy for DGs are provided. As well, some simple examples are done to confirm the proposed method. Then, the proposed method is applied to the microgrid for its SSS modal parameters extraction. Section 4 is the discussion, a framework based on the proposed method for the SSS identification, warning and emergency control online in microgrids is presented. The conclusions are summarized in Section 5.

2. Study on mall signal stability of microgrids

Although there are a few approaches for SSS of microgrids so far, their disadvantages are obviously. Therefore, a further work is strongly demand and a new field needs to be explored. In [26] a method for SSS of microgrids in interconnected mode had been proposed. A model presented in [27] is suitable for SSS of microgrids in isolated mode. They both featured the eigenvalue analysis approach as their theoretical basis and established SSS models in interconnected or isolated mode, respectively. However, results of eigenvalue approach for a fixed system may deviate far from the actual condition, due to the perturbation of system parameters, load fluctuations, power scheduling, distribution network disturbances and other causes of small disturbances in the real world. In addition, the calculation process of eigenvalues depends on system operation status strictly, unfortunately, which is hard to meet. The system's operation status varies frequently and largely, since the power outputs of wind turbines and photovoltaic arrays always vary in a large range slowly. As a result, it brings tremendous challenges to off-line SSS analysis based on eigenvalue analysis approach. What is more, conventional matrix eigenvalue approach is based on state space matrix obtained by the local linearization model of the complex nonlinear system. If we consider sophisticated control strategies as well as a number of nonlinear couplings, the eigenvalue approach will not be a good solution. Sometimes, the linearization model even may not be available. Besides, the interaction among different modes may cause new oscillation modes based on normal form theory [28–30]. Modes interaction is absolutely ignored by eigenvalue approach, because it is just the results of first-order Taylor expansion. Especially, its results of SSS arm to the whole system. As a result, we cannot know the specific modes for each DG or take emergency control strategies corresponding to the right DGs, when there are unstable modes in microgrids.

As mentioned previously, SSS of microgrids may be calculated by eigenvalue theory analytically, but there are some serious disadvantages. On the other hand, the SSS modal parameters of microgrids can also be identified or extracted by online data directly, which can overcome the disadvantage of eigenvalue analysis approach. This kind of methods has a wide range of applications in transmission network [31], although they also have some drawbacks. Common identification methods are Prony algorithm [32], Hilbert-Huang Transform (HHT) method [33] and the Matrix Pencil method [34,35], and so on. Traditional Prony algorithm uses complex exponential functions to fit the raw data, so it may produce a large number of false modes beside its sensitivity to noise. Although some improved iterative Prony algorithms can partially inhibit the effect of noise, they also increase the computation complexity [36–39]. HHT based modal identification method can extract the instantaneous modal information, but it results to a high computational complexity. Furthermore, its end effect needs to be overcome [40,41]. Matrix Pencil method is a typical signal recognition method, too. Recently, it has been applied to power system low frequency oscillation in [42], as it can overcome the noise interference and have low computational complexity [34,35]. Traditional Matrix Pencil method requires a threshold to obtain the modal order, which is depends on whether the ratio between each singular value and the largest one bigger than the threshold or not. How to set the threshold is affected by the size of raw data and the strength of noise, which is hard to be generalized and has no appropriate theoretical guidance.

A lot of relevant analysis showed that the key of the modal parameters extraction from raw data for SSS study is how to determine modal order accurately. If the modal order is few than its real value, it will miss some modes. In contrast, if the modal order is more, it will cause over-fit, which results to false modes and reduces the accuracy of the modal extraction results.

In this paper, Singular Entropy is proposed to determine the modal order of the raw data. It can not only obtain the modal order whether the noise affects the raw data or not, but also can remove the false modes and reduce computational complexity automatically. This method also uses Matrix Pencil method to extract the

modal parameters and analyze the SSS of the microgrids based on actual operation data in real world. So the SSS information of microgrids can be obtained real-time and online dynamically. It can adapt the operation status and small signal modes varying with time in microgrids. On the other hand, it can meet the demand for security and stability warning and emergency control.

3. Singular Entropy Matrix Pencil method and its microgrid application

3.1. Mathematical model of Singular Entropy Matrix Pencil method

Firstly, the Singular Entropy is presented to determine the order of the signal modes, which can accurately determine the modal order regardless of the noise. Then, Matrix Pencil method is used to extract the modal parameters of raw data. Combined with Singular Entropy and Matrix Pencil, the proposed method can remove the false modes and reduce computational complexity, automatically. The process can be described as follows.

3.1.1. Form Hankel matrix structure

The acquired or simulated raw data $y(i)$ ($i = 1, 2, \ldots, N$) can form a Hankel matrix:

$$\boldsymbol{Y} = \begin{bmatrix} y(1) & y(2) & \cdots & y(L+1) \\ y(2) & y(3) & \cdots & y(L+2) \\ \vdots & \vdots & \ddots & \vdots \\ y(N-L) & y(N-L+1) & \cdots & y(N) \end{bmatrix} \tag{1}$$

where L is the matrix pencil parameter and a proper chosen L can suppress noise in y. Take $L = N/4 \sim N/3$, usually. For $\boldsymbol{Y}$, we have $\boldsymbol{Y} = \boldsymbol{UDV}^T$ according to the singular value decomposed (SVD), where singular value matrix $\boldsymbol{D}$ is diagonal $\boldsymbol{D} \in \boldsymbol{R}^{(N-L)\times(L+1)}$. Its element σ_{ii} ($i = 1, 2, \ldots, m$) is the ith singular value of $\boldsymbol{Y}$, here $m = \min\{N-L, L+1\}$ is the minimum dimension of matrix $\boldsymbol{D}$. $\boldsymbol{U} \in \boldsymbol{R}^{(N-L)\times(N-L)}$ is the left eigenvector of $\boldsymbol{Y}$, while $\boldsymbol{V} \in \boldsymbol{R}^{(L+1)\times(L+1)}$ is the right one.

3.1.2. Determine the modal order

Singular Entropy had been introduced to detect fault in [43]. In this paper, we used it to extract the modal order of raw data y. Now, define the *Singular Entropy Increment*:

$$\Delta E_i = -\left(\frac{\sigma_{ii}}{\sum_{j=1}^{m}\sigma_{jj}}\right)\log\left(\frac{\sigma_{ii}}{\sum_{j=1}^{m}\sigma_{jj}}\right) \quad i = 1, 2, \ldots, m \tag{2}$$

where the kth order *Singular Entropy* E_k is defined as:

$$E_k = \sum_{i=1}^{k}\Delta E_i \quad k \le m \tag{3}$$

So the kth order *Differential of Singular Entropy Increment* is:

$$\Delta E_k' = \frac{\Delta E_k - \Delta E_{k-1}}{k-(k-1)} = \Delta E_k - \Delta E_{k-1} \quad k = 2, 3, \ldots, m \tag{4}$$

where $\Delta E_k'$ indicates the Differential of Singular Entropy Increment ΔE_k. When the effective signal saturates, the Singular Entropy Increment converges to a bounded value rapidly. So, there is an inflection point which is corresponding to the signal modal order. After that point, the Singular Entropy Increment is small, which can be considered as the effect of noise. Due to this advantage of Singular Entropy Increment, no matter how much the noise is, the increment of Singular Entropy will converge to a bounded value with a noticeable jump when the information of effective signal tends to saturation. With the help of Differential of Singular Entropy Increment, it is easy to extract the order of the corresponded inflection point, namely, the modal order n.

3.1.3. Form a new singular matrix

After we determined the modal order n, a new matrix $\boldsymbol{D}'$ can be formed by the first nth singular values of $\boldsymbol{D}$:

$$\boldsymbol{D}' = \begin{bmatrix} \sigma_1 & 0 & 0 & \cdots & 0 \\ 0 & \sigma_2 & 0 & \cdots & 0 \\ \vdots & \vdots & \vdots & \ddots & \vdots \\ 0 & 0 & 0 & \cdots & \sigma_n \\ \multicolumn{5}{l}{\mathbf{0}_{(N-L-n)\times n}} \end{bmatrix} \tag{5}$$

where $\boldsymbol{D}' \in \boldsymbol{R}^{(N-L)\times n}$, its first n rows are mainly formed by the first nth singular values of $\boldsymbol{D}$ and the last $N-L-n$ rows are zeros. The formed matrix $\boldsymbol{D}'$ can eliminate noise effectively, because it has removed the singular values caused by noise.

3.1.4. Obtain modal damping ratio and frequency

Now, form two matrixes $\boldsymbol{Y}_1$ and $\boldsymbol{Y}_2$:

$$\boldsymbol{Y}_1 = UD'\boldsymbol{V}_1^T \tag{6}$$

$$\boldsymbol{Y}_2 = UD'\boldsymbol{V}_2^T \tag{7}$$

where $\boldsymbol{V}_1$ is formed by the 1 to L rows of the right eigenvector $\boldsymbol{V}^T$ corresponding to first n singular values; $\boldsymbol{V}_2$ is formed by the 2 to $L+1$ rows of the right eigenvector $\boldsymbol{V}^T$ corresponding to first n singular values. Based on $\boldsymbol{Y}_1$ and $\boldsymbol{Y}_2$, a matrix pencil $\boldsymbol{Y}_2 - \lambda\boldsymbol{Y}_1$ can be derived. Modal parameters are included of the eigenvalues of matrix $\boldsymbol{G} = \boldsymbol{Y}_1^+\boldsymbol{Y}_2$, where $\boldsymbol{Y}_1^+$ is the pseudo-inverse matrix for $\boldsymbol{Y}_1$. If the number of non-zero eigenvalues for $\boldsymbol{G}$ is M, namely, $\lambda_i (i = 1, 2, \ldots, M; M \le n)$, the corresponding modal damping ratio and frequency of each mode can be obtained by Eqs. (8) and (9):

$$\xi_i = \frac{-sgn(Re(\lambda_i))}{\sqrt{1 + (Im(\ln\lambda_i/T_s)/Re(\ln\lambda_i/T_s))^2}} \tag{8}$$

$$f_i = \frac{Re(\ln\lambda_i/T_s)}{2\pi} \tag{9}$$

where λ_i is the ith eigenvalue of ith mode. ξ_i and f_i are the damping ratio and frequency of the ith mode, respectively. T_s is the sample time. According to Eq. (8), the system is unstable if any damping ratio ξ_i is negative. That is a simple judgement for SSS of microgrid.

3.2. Microgrid structure and control strategy

The structure diagram of a microgrid for study in this paper is shown in Fig. 1. It integrates 10 kW photovoltaic arrays (DG_1), 3 kW micro-gas turbine (DG_2) and 2 kW fuel cells (DG_3). There are some local loads at each DG's terminal, which are Load 1, Load 2 and Load 3, respectively. DGs are connected to the point of common coupling (PCC) by lines, where load 4 attached. Microgrid connected to utility grid at PCC simultaneously. The utility grid is a low voltage distribution network, whose rated root mean square value of phase-ground voltage is 220 V and its rated frequency is 50 Hz.

Conventional droop control of DG is shown in Fig. 2. According to the active and reactive power droop characteristics of DG, its decoupling control feature of frequency and potential amplitude can be achieved [44,45]. As shown in Fig. 2, the conventional droop control strategy can be expressed as:

$$\begin{cases} \omega = \omega_0 - k_p(P - P_{ref}) \\ E = E_0 - k_v(Q - Q_{ref}) \end{cases} \tag{10}$$

where ω and E are angular frequency and potential amplitude of the inverter, respectively. Meanwhile, ω_0 and E_0 are the ones correspond to the non-load situation. P and Q are the measured output

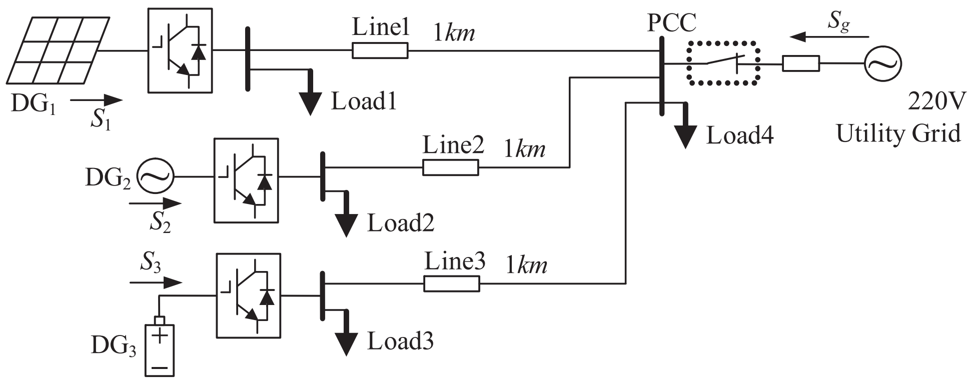


Fig. 1. The structure of a microgrid.

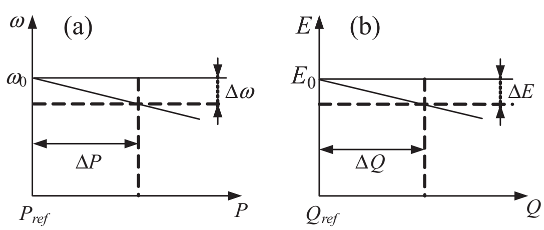


Fig. 2. Traditional droop control strategy of DG. (a) Active droop characteristic for frequency control. (b) Reactive droop characteristic for potential amplitude control.

active and reactive power components of the inverter. P_{ref} and Q_{ref} are the reference ones. k_p and k_v are the droop coefficients for the active and the reactive power.

The conventional droop control strategy works and coupling control can be achieved, when the line is inductive purely. However, if we take into account the resistive components, the angular frequency of DG will not only relative to the active power, but also reactive power [46]. These resistive components may be line resistance, the equivalent resistance of the filter inductance, parasitic resistance of the power electronic components and so on. Similar results can be reached for the potential amplitude [47]. On this situation, it is hard to decouple the complex and nonlinear system by the conventional droop control strategy as mentioned previously.

From (10), it is can be observed that the traditional droop control can be regarded as a Proportional Integral Derivative (PID) type controller, or just a proportional controller exactly, whose input is the active/reactive power deviations. In order to achieve the decoupling control of the microgrid with resistive components, we add an active, reactive power control cross and an integral component and the conventional droop controller or proportional controller [46,47]. Then, an improved droop control strategy is proposed, as shown in Fig. 3, where ω_f is the angular frequency for the filter whose transfer function is $G(s) = \omega_f/(s + \omega_f)$. $\tilde{P}$ and $\tilde{Q}$ are the active and reactive power after digital filter, respectively. $\boldsymbol{V}_{ref}$ is the reference voltage output of DG, which is given by

$$\begin{cases} \boldsymbol{V}_{refa} = E \sin(\omega t) \\ \boldsymbol{V}_{refb} = E \sin(\omega t - 2\pi/3) \\ \boldsymbol{V}_{refc} = E \sin(\omega t + 2\pi/3) \end{cases} \tag{11}$$

In Fig. 3, E_p is the potential of DG injected into the microgrid. P_{refi} and Q_{refi} are reference power outputs of DG_i, which is decided by the steady operation condition. $G_1(s)$ and $G_2(s)$ are the transfer functions of Proportional Integral (PI) regulators. In this paper, we take the follow expression:

$$\begin{cases} G_1(s) = k_{pp} + \dfrac{k_{pi}}{s} \\ G_2(s) = k_{qp} + \dfrac{k_{qi}}{s} \end{cases} \tag{12}$$

According to Fig. 3(a) and Eq. (12), the improved droop control strategy can be written as:

$$\begin{cases} \omega = \omega_0 + k_{pp}(P_{ref} - \tilde{P}) + k_{pi}\displaystyle\int_0^t (P_{ref} - \tilde{P})dt \\ + \left[k_{qp}(Q_{ref} - \tilde{Q}) + k_{qi}\displaystyle\int_0^t (Q_{ref} - \tilde{Q})dt\right] \\ E = E_0 + k_{qp}(Q_{ref} - \tilde{Q}) + k_{qi}\displaystyle\int_0^t (Q_{ref} - \tilde{Q})dt \\ - \left[k_{pp}(P_{ref} - \tilde{P}) + k_{pi}\displaystyle\int_0^t (P_{ref} - \tilde{P})dt\right] \end{cases} \tag{13}$$

The important parameters for the microgrid and controller are shown in Table 1. Notation that r and x_L are the parameters of lines, and the length of lines are shown in Fig. 1. The microgrid receives $S_g = 2 + j0.6$ kV A power from utility grid in the given steady-state condition according to power flow analysis. All DGs take the improved droop control strategy proposed.

Table 1
Parameters of the microgrid system.

Parameters	P_{ref1}	Q_{ref1}	P_{ref2}	Q_{ref2}	P_{ref3}	Q_{ref3}	P_g	Q_g
Values	10 kW	0.4 kvar	3 kW	0.4 kvar	2 kW	0.3 kvar	2 kW	0.6 kvar
Parameters	P_{L1}	Q_{L1}	P_{L2}	Q_{L2}	P_{L3}	Q_{L3}	P_{L4}	Q_{L4}
Values	5 kW	0.1 kvar	1 kW	0.5 kvar	1 kW	0.1 kvar	10 kW	1 kvar
Parameters	k_{pp}	k_{pi}	k_{qp}	k_{qi}	r	x_L	ω_0	E_0
Values	0.0005	0.0001	0.0001	0	0.243 Ω/km	0.83 Ω/km	314 rad/s	220 V

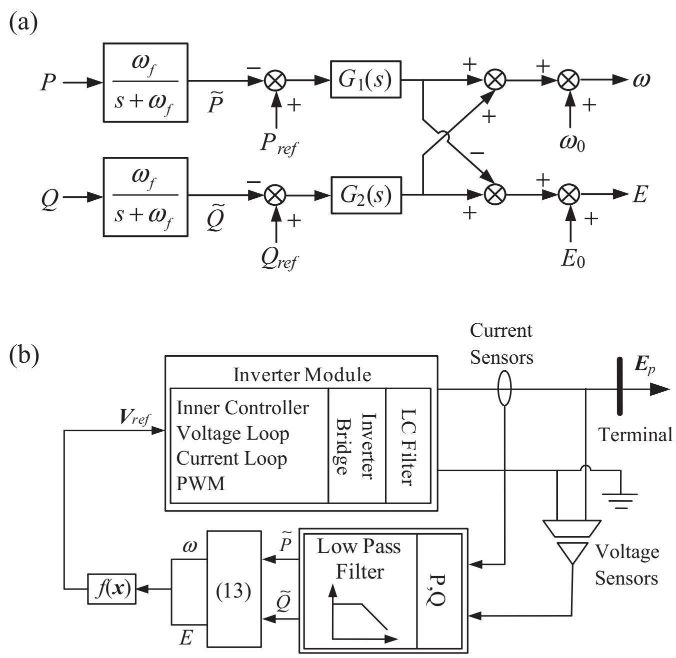


Fig. 3. The improved control strategy and structure of DG. (a) Block diagram for control strategy. (b) The control structure for hardware application of DG.

3.3. Simulation and results

3.3.1. Some simple examples

Now, we consider some simple examples, which can confirm the validity and effectiveness of the proposed method. If the active power $P(t)$ in per unit satisfies the following relationship:

$$P(t) = y(t) = y_1(t) + y_2(t) + y_3(t) + \varepsilon(t) \tag{14}$$

where $\varepsilon(t)$ is white noise. And the sample time is $T_s = 0.01$ s. Three oscillation signals with damping are expressed as:

$$y_1(t) = e^{-0.45t} \ \sin(20 \times 2\pi t) \tag{15}$$

$$y_2(t) = e^{-0.35t} \ \sin(2 \times 2\pi t) \tag{16}$$

$$y_3(t) = 0.2e^{-0.25t} \ \sin(0.5 \times 2\pi t) \tag{17}$$

There are three oscillation signals in $P(t)$, and each signal corresponds to the two modes in complex frame. So the accurate modal order is $2 \times 3 = 6$. When we consider the signal with noise, it is supposed that the white noise sequence meets normal distribution $\varepsilon(t) \sim N(0, \sigma)$. Fig. 4 shows the Singular Entropy Increment in case of $\sigma = 0$, $\sigma = 0.025$ and $\sigma = 0.05$, where "o" represents the turning point corresponding to the modal order of raw data. From Fig. 4, it is clear that the Singular Entropy Increment reflects the information of modal order accurately (both are 6). When we consider the signal without noise, the Singular Entropy Increment is zero after the modal order n. When we consider noise, the Singular Entropy Increment also has an apparent transition near the modal order n. After n, we regard these ΔE_k is caused by noise, which is very small and closed to a bounded value, approximately. So we can use Singular Entropy Increment to identify the modal order of raw signal.

3.3.1.1. Case 1: raw data without noise.

In this part, we consider the case that raw data is not polluted by noise, and give the modal parameters extraction results based on Singular Entropy Matrix Pencil. Fig. 5(a) gives the Singular Entropy Increment and its differential.

The modal order result from Singular Entropy Matrix Pencil is 6, and the signal noise ratio (SNR) for the fitting is $SNR = 585.68$ dB. In the same case, we use the Prony algorithm with 6 orders as a comparison. The results show that the signal noise ratio is $SNR = 151.19$ dB. Table 2 and Fig. 6 show the results in detail.

From Table 2 and Fig. 6, it is easy to find that the singular Entropy Matrix Pencil method can identify the modes of original signal well. In addition, it is more accurate than Prony algorithm. Especially, the phase result of Prony algorithm for mode 1 is far away from the accurate value, namely, the bold value as shown in Table 2.

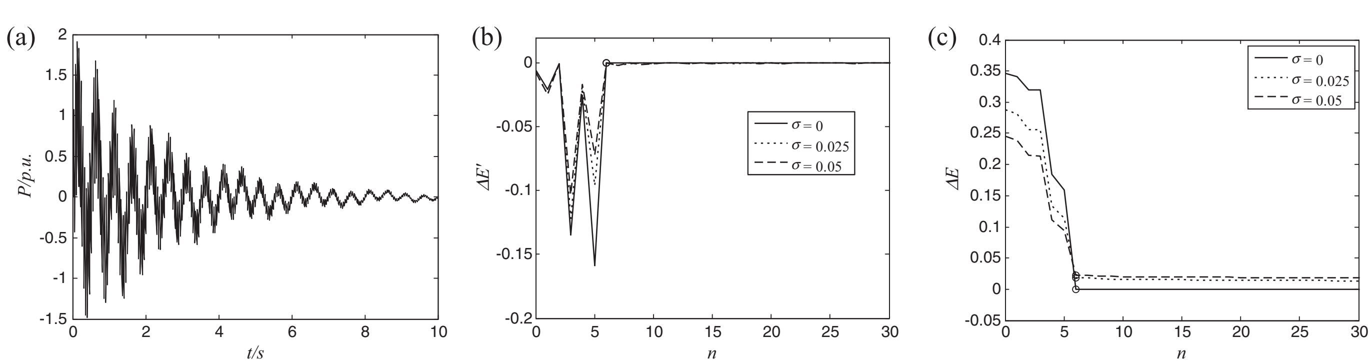


Fig. 4. Relationship between Singular Entropy Increment distribution and the modal order of raw data. (a) Raw data without noise in the time domain. (b) Differential of Singular Entropy Increment $\Delta E'$. (c) Singular Entropy Increment ΔE.

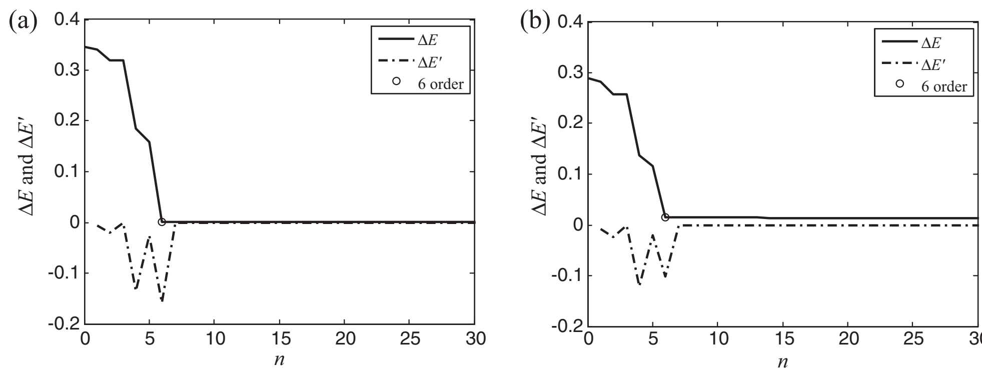


Fig. 5. Singular Entropy Increment and its differential to obtain the modal order. (a) The results for raw data without noise. (b) The results for raw data with noise.

Table 2
A comparison of identification results for raw data without noise.

	Frequency (Hz)		Damping ratio		Amplitude (p.u.)		Phase (rad)	
	Real	Identified	Real	Identified	Real	Identified	Real	Identified
Prony algorithm								
1	20	20.0001	0.0036	0.00358	1	1.0045	1.5708	**0.3142**
2	2	2.00078	0.0278	0.0278	1	1.0035	1.5708	1.4451
3	0.5	0.5016	0.0793	0.0793	0.2	0.2005	1.5708	1.5394
Singular Entropy Matrix Pencil								
1	20	20	0.0036	0.00358	1	1	1.5708	1.5708
2	2	2	0.0278	0.02784	1	1	1.5708	1.5708
3	0.5	0.5	0.0793	0.07933	0.2	0.2	1.5708	1.5708

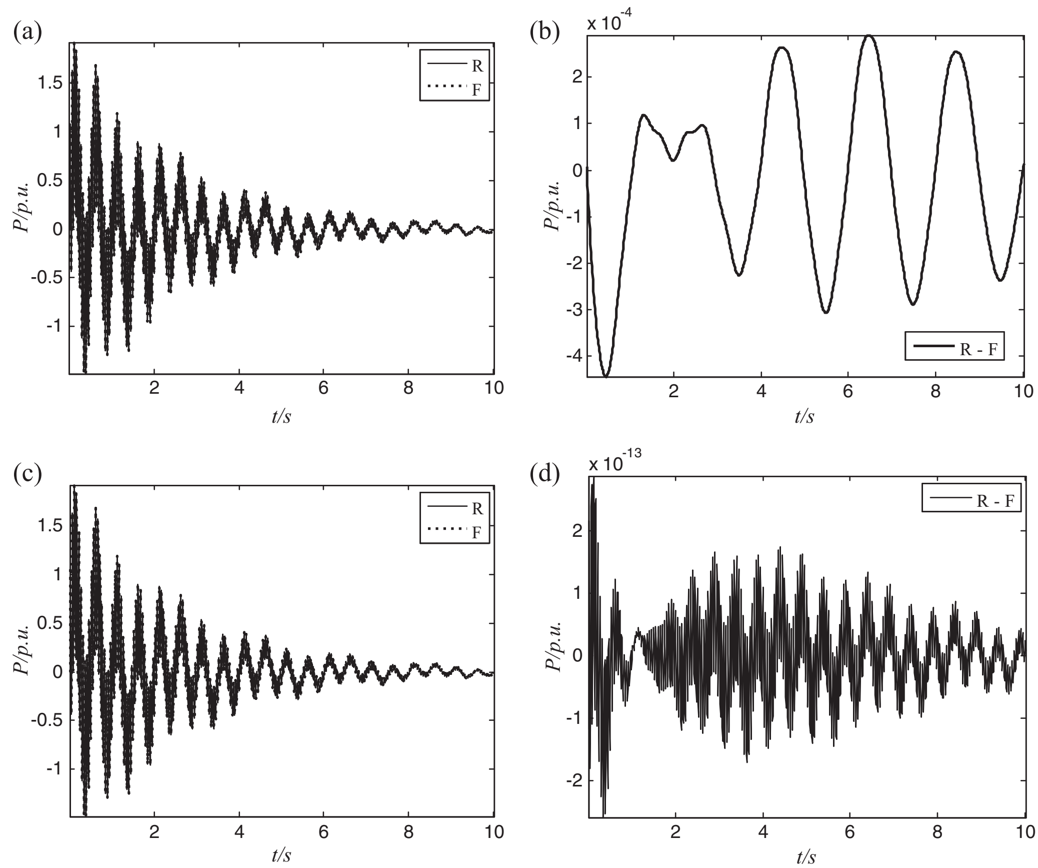


Fig. 6. The identification results for raw data without noise. (a) Comparison between raw data and fitting data by Prony algorithm. (b) Error for Prony algorithm (R–F). (c) Comparison between raw data and fitting data by Singular Entropy Matrix Pencil method. (d) Error for Singular Entropy Matrix Pencil method (R–F). R, raw data; F, fitting data.

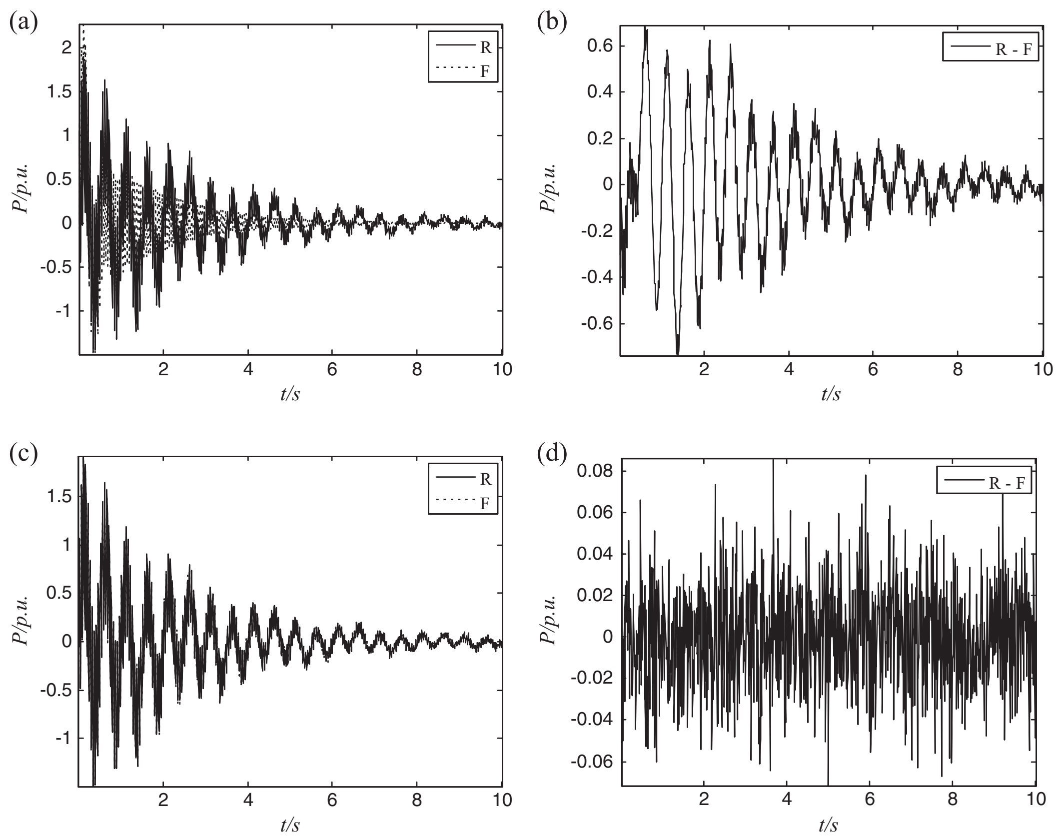


Fig. 7. The identification results for raw data with noise. (a) Comparison between raw data and fitting data by Prony algorithm. (b) Error for Prony algorithm (R–F). (c) Comparison between raw data and fitting data by Singular Entropy Matrix Pencil method. (d) Error for Singular Entropy Matrix Pencil method (R–F). R, raw data; F, fitting data.

When the raw data has no noise, the extracted modal parameters can meet some general requirements for simulation, such as oscillation modal identification, damping ratio analysis, evaluation of the rationality of the microgrid system structure, control equipment capacity and location planning and configuration, optimal design for control strategies and so on.

3.3.1.2. Case 2: raw data with noise. In this part, we consider the situation that the raw data in (14) has noise. We give modal identification results based on the Singular Entropy Matrix Pencil method and Prony algorithm. It is assumed that the noise meet $\varepsilon(t) \sim N(0, 0.025)$. Fig. 5(b) shows the changes for Singular Entropy Increment and its differential, while the "o" refers to the modal order identified. It is easy to see that Singular Entropy Matrix Pencil method can get the modal order exactly.

When $\sigma = 0.025$, we can identify that the modal order of signal is 6 by Singular Entropy Matrix Pencil, and the signal noise ratio for fitting is $SNR = 53.51$ dB. Prony algorithm with actual modal order is used as a comparison, while its *SNR* is 9.49 dB. A comparison of identification results is shown in Table 3 and Fig. 7. Table 3 shows that the identified results of Prony algorithm are still poor due to its sensitivity to noise even if the correct modal order is used.

From the comparison of Table 3 and Fig. 7, since Singular Entropy Matrix Pencil can exclude false modes, its identification results are very close to the actual signal. From Fig. 5, it is clear that the Singular Entropy Increment of the belt in case 2 become a little worse compared with case 1 because of the noise. Although, two methods can extract the modal parameters exactly in case 1 without noise. In case 2, the Singular Entropy Matrix Pencil method performances well while Prony algorithm is failed.

3.3.2. Applied Singular Entropy Matrix Pencil method into microgrid

A microgrid simulation model is established based on the microgrid structure shown in Fig. 1 and the proposed control strategy in

Table 3
A comparison of identification results for raw data with noise.

	Frequency (Hz)		Damping rate		Amplitude (p.u.)		Phase (rad)	
	Real	Identified	Real	Identified	Real	Identified	Real	Identified
Prony algorithm								
1	20	20	0.0036	0.0046	1	1.13	1.571	0.181
2	2	2	0.0278	0.223	1	1. 91	1.571	1.429
3	0.5	–	0.0793	–	0.2	–	1.571	–
Singular Entropy Matrix Pencil								
1	20	20	0.0036	0.0036	1	1	1.571	1.568
2	2	2	0.0278	0.0278	1	0.99	1.571	1.568
3	0.5	0.5	0.0793	0.0752	0.2	0.19	1.571	1.564

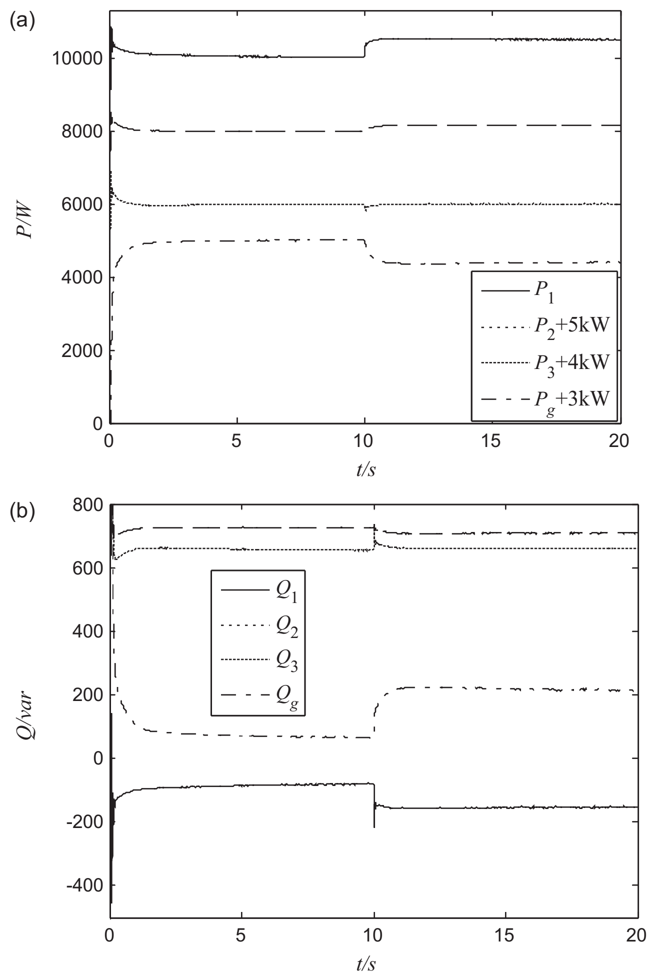


Fig. 8. The power outputs of each DG and utility grid. (a) Active power; (b) reactive power.

Fig. 3. The parameters of the microgrid are shown in Table 1. In this part, Singular Entropy Matrix Pencil method is applied to analyze its SSS. Supposed that the microgrid is in interconnected operated mode, and the results in isolated mode can be obtained analogously. The small disturbance is set that the DG_1 has a 5% active power step disturbance at 10 s.

Active power signals are chosen for modal extraction because they reflect the dynamic of voltage, current and power angle directly. The power outputs of each DG are shown in Fig. 8. We extract the modal parameters of the system by each DG's active power signal P_i (i = 1, 2, 3) and utility grid power P_g in the time domain 10–18 s. The sample time is T_s = 0.01 s. The identification results are shown in Figs. 9–12. And the main oscillation modes for each signal are shown in Table 4.

Table 4
The main modes of each DG extracted by Singular Entropy Matrix Pencil.

Active power	*SNR* (dB)	Frequency (Hz)/damping ratio
P_1	168.24	0.318/0.107, 17.681/0.231
P_2	155.00	0.355/0.020, 5.720/0.636, 17.767/0.184
P_3	147.457	0.356/0.016, 5.658/0.621, 16.944/0.209
P_g	120.242	0.327/0.051, 0.594/0.049, 18.261/0.513

According to Table 4, it can be observed that the damping ratio of each mode is positive, that is, the system has no positive real eigenvalue and the system is stable. It is worth to notice that each DG has high frequency oscillation modes whose frequency is larger than 5 Hz. These modes reflect the rapid transient after system disturbance. On the other hand, each DG has low frequency oscillation modes whose frequency is less than 5 Hz. Notation that these damping ratios corresponding to low frequencies are small. Thus, these modes may be more dangerous and easy to be unstable when system operation status changes. The DGs have different main oscillation modes, and that cannot be obtained by eigenvalue analysis.

4. Discussion

The stability of microgrids is the basic requirement for a safe and reliable distributed power delivery system. Unfortunately, there are a few researches on it. Similar to the transmission network, the stability for microgrids is divided into small disturbance stability and transient stability too. However, the operation conditions of photovoltaic arrays and wind turbines depend on meteorological conditions highly. Their stochastic, intermittent and time-variant characteristics lead to the power outputs of renewable sources change frequently. These can be considered as small disturbances. Visibly, small disturbances are so frequent that the SSS is very complex and important in microgrids.

Conventional SSS approaches mainly use the local linearized state space model of the nonlinear system. Then the SSS results can be obtained by eigenvalues analysis. If all the eigenvalues are scattered beside left coordinate in the complex plane, the system is stable. On the contrary, if there has a positive real part eigenvalue, then the system is unstable. However, due to the unique characteristics of photovoltaic arrays and wind turbines, the linearized model is time-variant frequently even hard to get. Therefore, such an approach is greatly flawed for SSS of microgrids. In the other word, a further work is strongly demand and a new field need to be explored for SSS of microgrids.

In this paper, a new method for SSS of microgrids is proposed, which can extract the modal parameters from the observed raw data. It is verified by some simple examples and a microgrid with improved droop control strategy. According to the proposed approach, the system is unstable, if there is any mode with negative

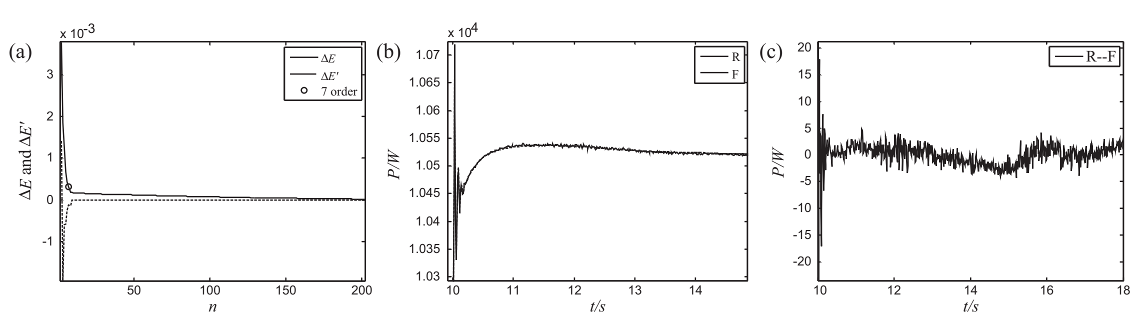


Fig. 9. Modal parameters extracted using active power of DG1 (P1). (a) Singular Entropy Increment and its differential to get the modal order. (b) Comparison between raw data and fitting data by Singular Entropy Matrix Pencil method. (c) Error for Singular Entropy Matrix Pencil method (R–F). R, raw data; F, fitting data.

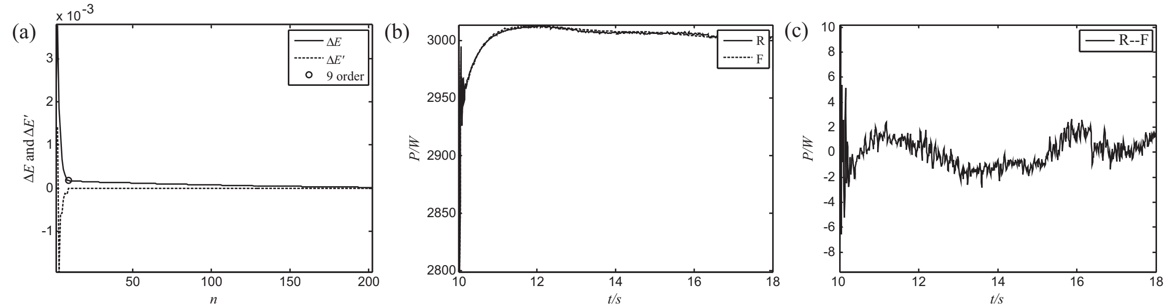


Fig. 10. Modal parameters extracted using active power of DG2 (P2). (a) Singular Entropy Increment and its differential to get the modal order. (b) Comparison between raw data and fitting data by Singular Entropy Matrix Pencil method. (c) Error for Singular Entropy Matrix Pencil method (R–F). R, raw data; F, fitting data.

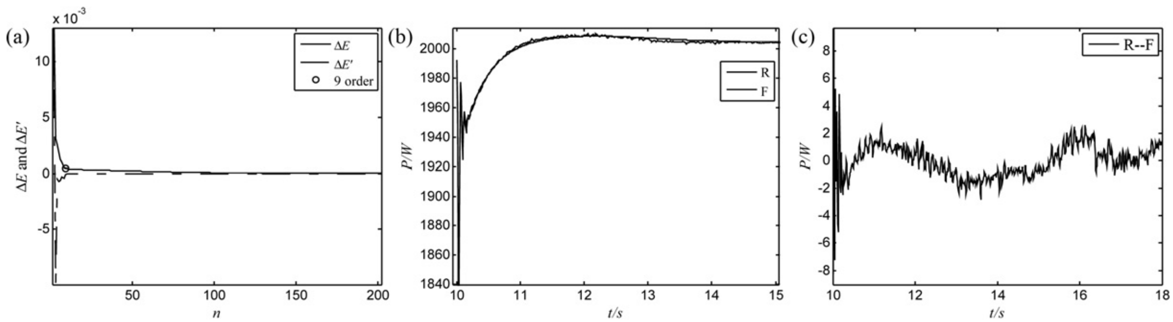


Fig. 11. Modal parameters extracted using active power of DG3 (P3). (a) Singular Entropy Increment and its differential to get the modal order. (b) Comparison between raw data and fitting data by Singular Entropy Matrix Pencil method. (c) Error for Singular Entropy Matrix Pencil method (R–F). R, raw data; F, fitting data.

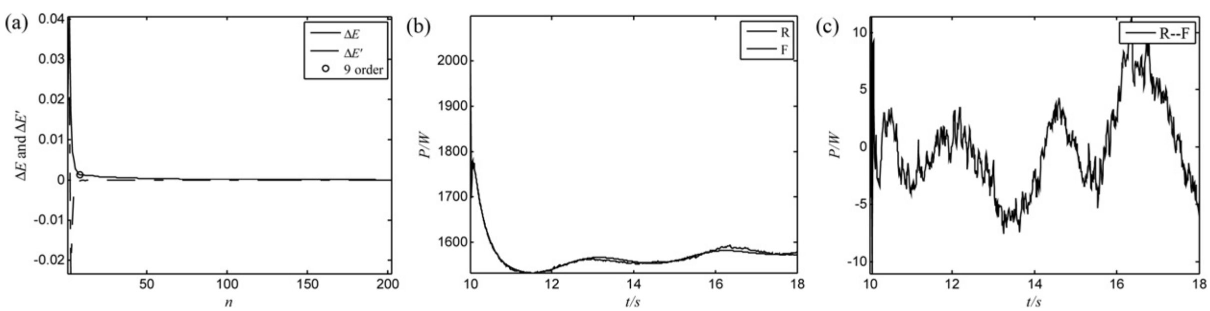


Fig. 12. Modal parameters extracted using active power of utility grid side (P_g). (a) Singular Entropy Increment and its differential to get the modal order. (b) Comparison between raw data and fitting data by Singular Entropy Matrix Pencil method. (c) Error for Singular Entropy Matrix Pencil method (R–F). R, raw data; F, fitting data.

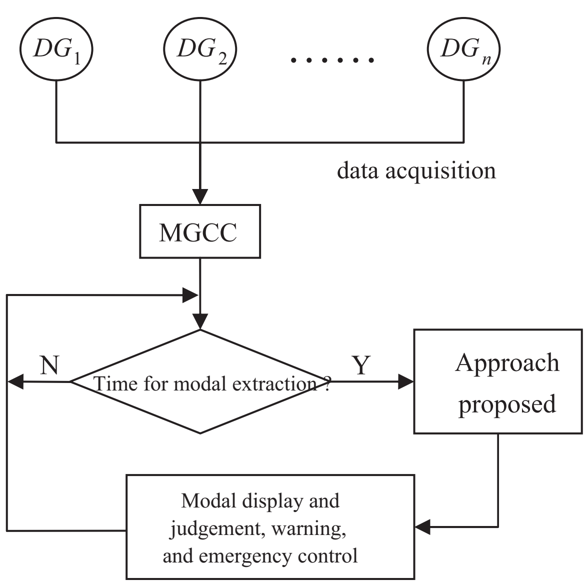


Fig. 13. An application framework integrated the proposed approach in microgrids.

damping which corresponds a positive real part eigenvalue. Thus, this approach can be applied to extract the SSS modal information real-time and online, warn and emergency control in microgrids. The framework is shown in Fig. 13 and the processes can be described as follows:

1. Required active power data be measured in the terminal of DGs firstly. Then, the raw data is transmit to microgrid control center (MGCC).
2. After MGCC obtains a certain number of raw data points, modal parameters can be extracted by the proposed approach.
3. According to the modal parameters, if there is any mode with negative damping ratio or the damping ratio is less than a positive threshold, the microgrid is judged as unstable or near to unstable. Thus, some emergency control strategies should be taken or warning should be given according to the contingency plans.

5. Conclusions

In microgrids, the SSS should attract more attention because of the unique characteristics of photovoltaic arrays and wind

turbines. This paper gives a review on SSS of microgrids and proposes a new SSS method based on Singular Entropy and Matrix Pencil. Furthermore, a microgrid simulation model with an improved control strategy is used to verify it. Some conclusions could be summarized as follows:

1. SSS of microgrid is a very important issue of microgrids due to the unique characteristics of renewable sources, while there are rarely researches on it.
2. Singular Entropy Matrix Pencil method uses the raw data acquired from microgrids. So it can get its real-time and online SSS information dynamically.
3. The proposed method applies Singular Entropy theory to extract the actual modal order exactly. It can exclude false modes, reduce the computational complexity and improve the accuracy. Besides, it combines with Matrix Pencil which can overcome the signal noise very well and extract modal parameters accurately.
4. Simulation results have proved the feasibility, validity and accuracy of the presented method. It shows that the proposed approach is suitable for SSS of microgrids and the signal noise ratio between fitting data and the raw data is high.
5. A framework of the proposed approach for modal parameters extraction, monitoring, warning, and emergency control in microgrids is given.

Acknowledgments

The financial support from National Natural Science Foundation of China (No. 50907060) and China Postdoctoral Science Foundation funded project (20090451438), the help from Yizhe Xu (graduate student in Department of Electrical and Computer Engineering, North Carolina State University) and Dr. Qingfen Liao (in School of Electrical Engineering, Wuhan University) are gratefully acknowledged.

References

[1] Carreras BA, Newman DE, Dobson I, Poole AB. Initial evidence for self-organized criticality in electric power system blackouts. In: Proceedings of the 33rd Annual International Conference on System Sciences, IEEE. 2000, January. p. 6, doi:10.1109/HICSS.2000.926768.

[2] Carreras BA, Newman DE, Dobson I, Poole AB. Evidence for self-organized criticality in a time series of electric power system blackouts. IEEE Transactions on Circuits and Systems – I: Regular Papers 2004;51(September (9)):1733–40, doi:10.1109/TCSI.2004.834513.

[3] Su S, Li YH, Duan XZ. Self-organized criticality of power system faults and its application in adaptation to extreme climate. Chinese Science Bulletin 2009;54(February (7)):1251–9, doi:10.1007/s11434-009-0087-5.

[4] Lasseter RH, Paigi P. Microgrid: a conceptual solution. In: IEEE Power Electronics Specialists Conference. 2004, June. p. 4285–90, doi:10.1109/PESC.2004.1354758.

[5] Lasseter RH. Microgrids and distributed generation. Journal of Energy Engineering 2007;133(September (3)):144–9, doi:10.1061/(ASCE)0733-9402.

[6] Barnes M, Kondoh J, Asano H, Oyarzabal J, Ventakaramanan G, Lasseter R, et al. Real-world microGrids – an overview. In: IEEE International Conference on System of Systems Engineering. 2007, April. p. 8, doi:10.1109/SYSOSE.2007.4304255.

[7] Kavasseri RG, Nagarajan R. A multifractal description of wind speed records. Chaos Solitons & Fractals 2005;24(April (1)):165–73, doi:10.1016/j.chaos.2004.09.004.

[8] Lakshmanan N, Gomathinayagam S, Harikrishna P, Abraham A, Ganapathi SC, Ganapathi SC. Basic wind speed map of India with long-term hourly wind data. Current Science 2009;96(April (7)):911–22.

[9] Kavasseri RG, Nagarajan R. Evidence of crossover phenomena in wind-speed data. IEEE Transactions on Circuits and Systems – I: Regular Papers 2004;51(November (11)):2255–62, doi:10.1109/TCSI.2004.836846.

[10] Bilbao E, Gaztanaga H, Mir L, Etxeberria-Otadui I, Milo A. Design and development of a supercapacitor-based microgrid dynamic support system. In: IEEE 13th European Conference on Power Electronics and Applications. 2009, September. p. 10.

[11] Lidula NWA, Rajapakse AD. Microgrids research: a review of experimental microgrids and test systems. Renewable and Sustainable Energy Reviews 2011;15(1):186–202, doi:10.1016/j.rser.2010.09.041.

[12] Lasseter R, Akhil A, Marnay C, Stevens J, Dagle J, Guttromson R, et al. The CERTS microgrid concept, http://www.pserc.org/ecow/get/researchdo/certsdocum0/certspubli/certsmicrogridwhitepaper.pdf; 2002, April.

[13] Nichols DK, Stevens J, Lasseter RH, Eto JH, Vollkommer HT. Validation of the CERTS microgrid concept the CEC/CERTS microgrid testbed. In: Power Engineering Society General Meeting. 2006, June. p. 3, doi:10.1109/PES.2006.1709248.

[14] Morais H, Kádár P, Faria P, Vale ZA, Khodr HM. Optimal scheduling of a renewable micro-grid in an isolated load area using mixed-integer linear programming. Renewable Energy 2010;35(January (1)):151–6, doi:10.1016/j.renene.2009.02.031.

[15] Kroposki B, Lasseter R, Ise T, Morozumi S, Papatlianassiou S, Hatziargyriou N. Making microgrids work. Power and Energy Magazine 2008;6(June (3)):40–53, doi:10.1109/MPE2008918718.

[16] Lopes JAP, Moreira CL, Madureira AG. Defining control strategies for microgrids islanded operation. IEEE Transactions on Power Systems 2006;21(May (2)):916–23, doi:10.1109/TPWRS.2006.873018.

[17] Lopes JAP, Moreira CL, Resende FO. Control strategies for microgrids black start and islanded operation. International Journal of Distributed Energy Resources 2005;1(July (3)).

[18] Li X, Song Y, Han S. Frequency control in micro-grid power system combined with electrolyzer system and fuzzy PI controller. Journal of Power Sources 2008;180(May (1)):468–75, doi:10.1016/j.jpowsour.2008.01.092.

[19] Obara S. Load response characteristics of a fuel cell micro-grid with control of number of units. International Journal of Hydrogen Energy 2006;31(October (13)):1819–30, doi:10.1016/j.ijhydene.2006.05.004.

[20] Uzunoglu M, Onar OC, Alam MS. Modeling, control and simulation of a PV/FC/UC based hybrid power generation system for stand-alone applications. Renewable Energy 2009;34(March (3)):509–20, doi:10.1016/j.renene.2008.06.009.

[21] Kariniotakis GN, Soultanis NL, Tsouchnikas AI, Papathanasiou SA, Hatziargyriou ND. Dynamic modeling of microgrids. In: IEEE International Conference on Future Power Systems. 2005, November. p. 7, doi:10.1109/FPS.2005.204227.

[22] Kim S, Jeon J, Cho C, Kim E, Ahn J. Modeling and simulation of a grid-connected PV generation system for electromagnetic transient analysis. Solar Energy 2009;83(May (5)):664–78, doi:10.1016/j.solener.2008.10.020.

[23] Li YH, Choi SS, Rajakaruna S. An analysis of the control and operation of a solid oxide fuel-cell power plant in an isolated system. IEEE Transactions on Energy Conversion 2005;20(June (2)):381–7, doi:10.1109/TEC.2005.847998.

[24] Jyung TY, Baek YS, Kim YG. Improvement of a power quality of microgrid system interconnected to distribution system in emergency condition. In: IEEE Transmission & Distribution Conference & Exposition: Asia and Pacific. 2009, October. p. 1–4, doi:10.1109/TD-ASIA.2009.5357000.

[25] Vokony I, Dán A. Creation of stability index for micro grids. In: International Conference on Renewable Energies and Power Quality. European Association for the Development of Renewable Energies, Environment and Power Quality (EA4EPQ); 2010, March. p. 1–4.

[26] Katiraei F, Iravani MR, Lehn PW. Small-signal dynamic model of a micro-grid including conventional and electronically interfaced distributed resources. Generation, Transmission & Distribution, IET 2007;1(March (30)):369–78, doi:10.1049/iet-gtd:20045207.

[27] Xiao ZX, Wang CS, Wang SX. Small-signal stability analysis of microgrid containing multiple micro sources. Automation of Electric Power Systems 2009;33(March (6)):81–5.

[28] Thapar J, Vittal V, Kliemann W, Fouad AA. Application of the normal form of vector fields to predict interarea separation in power systems. IEEE Transactions on Power Systems 1997;12(May (2)):844–50, doi:10.1109/59.589716.

[29] Gilsoo J, Vittal V, Kliemann W. Effect of nonlinear modal interaction on control performance: use of normal forms technique in control design. I. General theory and procedure. IEEE Transactions on Power Systems 1998;13(May (2)):401–7, doi:10.1109/59.667359.

[30] Gilsoo J, Vittal V, Kliemann W. Effect of nonlinear modal interaction on control performance: use of normal forms technique in control design. II. Case studies. IEEE Transactions on Power Systems 1998;13(May (2)):408–13, doi:10.1109/59.667360.

[31] Venayagamoorthy GK, Aliyu UO, Chow JH, Sanchez-Gasca JJ. Modal extraction with three different methods for the Nigerian power system. In: Int. Conference on Power System Operation and planning-VI. 2005, May. p. 61–6.

[32] Hauer JF, Demeure CJ, Scharf LL. Initial result in prony analysis of power system response signals. IEEE Transactions on Power Systems 1990;5(February (1)):80–9, doi:10.1109/59.49090.

[33] Messina AR, Vittal V. Nonlinear, non-stationary analysis of interarea oscillations via Hilbert spectral analysis. IEEE Transactions on Power Systems 2006;21(August (3)):1234–41, doi:10.1109/TPWRS.2006.876656.

[34] Hua Y, Sarkar TK. On SVD for estimating generalized eigenvalues of singular matrix pencil in noise. IEEE Transactions on Signal Processing 1991;39(April (4)):892–900, doi:10.1109/78.80911.

[35] Hua Y. Parameter estimation of exponentially damped sinusoids using higher order statistics and matrix pencil. IEEE Transactions on Signal Processing 1991;39(July (7)):1691–2, doi:10.1109/78.134411.

[36] Osborne MR, Smyth GK. A modified Prony algorithm for exponential function fitting. SIAM Journal on Scientific Computing 1995;16(January (1)):119–38.

[37] Kundu D. A modified Prony algorithm for sum of damped or undamped exponential signals. Sankhyā: The Indian Journal of Statistics, Series A 1994;56(3):524–44.

[38] Dupuis P, Sels T, Driesen J, Belmans R. Exponential parameters measurement using a modified prony method. In: IEEE IMTC 2004 – Instrumentation and Measurement. 2004, May. p. 1590–4, doi:10.1109/IMTC.2004.1351386.

[39] Steedly W, Ying CJ, Moses OL. A modified TLS-Prony method using data decimation. IEEE Transactions on Signal Processing 1994;42(September (9)):2292–303, doi:10.1109/78.317852.

[40] Huang NE. Hilbert-Huang transform and its applications. World Scientific Publishing Company; 2005.

[41] Dätig M, Schlurmann T. Performance and limitations of the Hilbert-Huang transformation (HHT) with an application to irregular water waves. Ocean Engineering 2004;31(October (14–15)):1783–834.

[42] Crow ML, Singh A. The matrix pencil for power system modal extraction. IEEE Transactions on Power Systems 2005;20(February (1)):501–2, doi:10.1109/TPWRS2004841158.

[43] He ZY, Fu L, Lin S, Bo ZQ. Fault detection and classification in EHV transmission line based on wavelet singular entropy. IEEE Transactions on Power Delivery 2010;25(4):2156–63, doi:10.1109/TPWRD.2010.2042624.

[44] De Paiva EP, Vieira JB, De Freitas LC, Farias VJ, Coelho EAA. Small signal analysis applied to a single phase inverter connected to stiff AC system using a novel improved power controller. In: 20th Annual IEEE Applied Power Electronics Conference and Exposition. 2005, March. p. 1099–104, doi:10.1109/APEC.2005.1453133.

[45] Tuladhar A, Jin H, Unger T, Mauch K. Parallel operation of single phase inverter modules with no control interconnections. In: 12th IEEE Annual Applied Power Electronics Conference and Exposition. 1997, February. p. 94–100, doi:10.1109/APEC.1997.581439.

[46] Chen LL, Xiao L, Gong CY, Yan YG. Circulating current's characteristics analysis and the control strategy of parallel system based on double close-loop controlled VSI. In: 35th Annual IEEE Power Electronics Specialists Conference. 2004. p. 4791–7, doi:10.1109/PESC.2004.1354846.

[47] Guerrero JM, de Vicuna LG, Matas J, Castilla M, Miret J. A wireless controller to enhance dynamic performance of parallel inverters in distributed generation systems. IEEE Transactions on Power Electronics 2004;19(September (5)):1205–13, doi:10.1109/TPEL.2004.833451.